THE ASTRONOMICAL JOURNAL, 116:2438–2442, 1998 November

NEWLY DISCOVERED HERBIG-HARO OBJECTS IN BARNARD 1 AND NGC 1333

JUN YAN,[1,2] HONGCHI WANG,[1,2] MIN WANG,[1,2] LICAI DENG,[1,3] JI YANG,[2] AND JIANSHENG CHEN[1,3]
Received 1998 April 24; revised 1998 July 10

ABSTRACT

We have carried out a wide-field survey for Herbig-Haro (HH) objects in nearby star-forming regions using the Beijing Astronomical Observatory 60/90 cm Schmidt telescope. The survey covered 56 deg^2 in Perseus, Taurus, Orion, Monoceros, and other regions. Here we report our discovery of seven HH objects (HH 427–433) in the Barnard 1 dark cloud and one HH object (HH 426) in NGC 1333. The newly discovered HH objects demonstrate a great variety of morphological structures: HH 426, 429, and 432 each consist of two knots, HH 427 is a single knot, HH 428 is a bar, HH 430 is a jet, HH 431 is a bow shock–shaped patch, and HH 433 is a complex of four knots. HH 432A, 432B, and 433 constitute a giant, highly collimated jet with a projected linear size of $\sim$0.5 pc and a collimation ratio of $\sim$11. The jet aligns well with a nearby star, IRAS 03304+3100 (LkHα 327), and may be driven by this source. Two optically visible stars are supposed to be the exciting sources for HH 426 and 428. For HH 427, 429, and 430, no exciting source can be identified.

Key words: ISM: Herbig-Haro objects — ISM: jets and outflows — ISM: individual (Barnard 1, NGC 1333) — stars: formation — stars: pre–main-sequence

1. INTRODUCTION

Herbig-Haro (HH) objects are shock-excited nebulae intimately associated with star-forming regions (Schwartz 1978). Like CO molecular outflows and shock-excited near-IR emissions of H_2, HH objects are good tracers of the mass outflow activities of young stellar objects (YSOs) (Reipurth & Cernicharo 1995). The prototypical HH objects, HH 1 and 2, were discovered by Herbig (1951) and Haro (1952). Since then, more than 400 HH objects have been found by several search methods, including objective-prism Schmidt survey, narrowband CCD imaging, near-IR imaging, and other methods (Reipurth 1994).[4]

We have carried out a large-field Schmidt CCD survey of HH objects using a combination of intermediate-band and narrowband filters. The survey covered star-forming regions in the local molecular clouds of Perseus, Taurus, Orion, Monoceros, and other regions. In the survey we discovered seven HH objects in Barnard 1 and one HH object in NGC 1333.

Barnard 1 (B1) is a dark cloud located in the local Perseus complex at a distance of 350 pc. Six HH objects (Alten et al. 1997), three CO outflows (Bachiller, Menten, & del Rio-Alvarez 1990; Bachiller, Martin-Pintado, & Planesas 1991) have been found in this region. Ladd, Lada, & Myers (1993) observed some *IRAS* sources in this region in the infrared H and K bands and found that IRAS 03271+3013 is a Class I object. Bachiller et al. (1990) observed B1 in the CS $J = 1$–0 line and (1, 1) and (2, 2) NH_3 lines. The CS emission reveals a dense region of size $\sim(2 \times 5)$ pc, with a mass of $\sim$1200 $M_\odot$. The NH_3 lines show evidence for two clumps of size $\sim$0.07 and $\sim$0.21 pc and masses greater than 0.4 and 13 $M_\odot$, respectively.

NGC 1333 is a reflection nebula in the Perseus molecular complex and is associated with a region of recent star formation. Several groups of HH objects (HH 4–18) were discovered by Herbig (1974). Bally, Devine, & Reipurth (1996) found over 20 groups of HH objects (HH 333–353), including a spectacular jet (HH 333). A cluster of about 150 low- to intermediate-mass YSOs (Aspin, Sandell, & Russell 1994; Lada, Alves, & Lada 1996), many far-infrared objects (Jennings et al. 1987), some Class 0 sources (Sandell et al. 1991, 1994), a complex of overlapping CO outflows (Liseau, Sandell, & Knee 1988), and highly obscured shocks visible in the 2.122 μm H_2 line (Hodapp & Ladd 1995) have been found in the NGC 1333 region.

2. OBSERVATIONS

The observations were carried out at Xinglong Station of Beijing Astronomical Observatory (BAO). The telescope used is the BAO f/3 60/90 cm Schmidt telescope equipped with a 2048 × 2048 Aerospace Ford CCD that has a field of view of 57′ × 57′. The pixel size is 15 μm, corresponding to a resolution of 1.″67 pixel^{-1} (Fan et al. 1996). The filter set used in this program is made up of two BATC[5] intermediate-band filters [BATC09], [BATC10], and a narrowband filter [S II]. The parameters of the filters are given in Table 1. As shown in the table, the [BATC09] filter covers well the strong and characteristic lines of HH objects, while the [BATC10] band covers no strong line of HH objects and, therefore, is used to measure the continuum.

For the purpose of a large-field survey of HH objects in star-forming regions, we selected observation fields in the survey based on the following selection criteria: there are any known HH objects, molecular outflows, H_2O or OH masers, *IRAS* sources of Class 0 or Class I, and GGD

[1] Beijing Astronomical Observatory, Chinese Academy of Science, 15 Zhongguancun, Beijing 100080, China.
[2] Purple Mountain Observatory, Chinese Academy of Science, 2 Beijing Xi Lu, Nanjing, Jiangsu 210008, China.
[3] Chinese Academy of Sciences–Peking University: Beijing Astrophysics Center.
[4] See ftp://ftp.hq.eso.org/pub/Catalogs/Herbig-Haro.
[5] The Beijing-Arizona-Taiwan-Connecticut Multicolor Sky Survey.

TABLE 1

FILTER PARAMETERS

Filter	Central Wavelength (Å)	Band width (Å)	Property
[BATC09].....	6660	480	[N II], H_α, [S II]
[BATC10].....	7050	300	Continuum
[S II]	6725	50	[S II] $\lambda\lambda$6717, 6731

(Gyulbudaghian, Glushkov, & Denisyuk 1978) or RNO (Cohen 1980) objects in or near the fields. Our survey sequence includes a first-step quick survey for HH candidates and a narrowband identification. For a target field, three or more frames in both [BATC09] and [BATC10] bands were taken so that the cosmic rays and the bad pixels could be removed. We conducted bias subtraction, dome flat-field normalization, and image combination using the IRAF package. HH object candidates were picked up by their presence in the [BATC09] images and absence in the [BATC10] images.

After the first step, there is some possibility of contamination by bright rims of H II regions and reflection nebulae. In the second step we used the narrowband [S II] filter to identify HH objects. Three frames, each with an exposure time of 20 minutes, were taken. The frames were reduced just as in the [BATC09] and [BATC10] bands. The HH objects were identified by their presence in the [S II] images and absence in the [BATC10] images.

We observed three fields in the region of B1 and NGC 1333. The [BATC09] and [BATC10] observations were made during 1995 October 24–25, and the [S II] observations were made during 1996 December 7–8. The seeing was around 2″ during the observations. Table 2 gives the log of observations. In this region we found that more than 90% of the candidate HH objects from our first step could be identified in the [S II] band. The images of HH objects are sharper in the [S II] frames than in the [BATC09] frames.

3. RESULTS AND DISCUSSION

In the fields toward B1 and NGC 1333, we discovered seven HH objects in B1 and one HH object in NGC 1333. Their coordinates in the B1950.0 epoch are listed in Table 3. The astrometry was done by using the Guide Star Catalog (GSC). We registered the brighter stars in each image with the GSC coordinate system. Centroids of all the GSC stars in an image, typically greater than 100 stars, are used to determine the plate solution. Our astrometric accuracy is comparable to the GSC system (Fan et al. 1996).

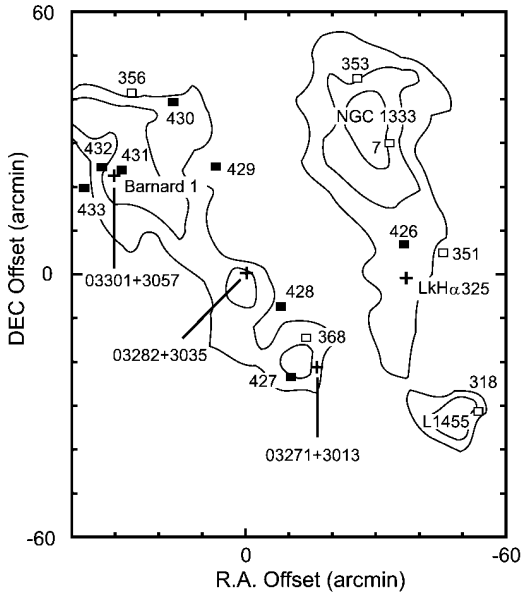

FIG. 1.—Schematic representation of the locations of HH 426–433 in Barnard 1 and NGC 1333. Some of the known HH objects and outflows in this region are also marked. The newly found HH objects are marked with filled rectangles. The known HH objects and outflows are marked with open rectangles and plus signs, respectively. The contours of the ^{13}CO $J = 1$–0 line emission are taken from Bachiller & Cernicharo (1986). Position offsets are with respect to the *IRAS* position of IRAS 03282+3035 ($\alpha = 03^h28^m15^s.2$, $\delta = 30°35'14''$; B1950.0).

The locations of the newly found HH objects in B1 and NGC 1333 are illustrated in Figure 1. In the figure some of the known HH objects and outflows in this region are also indicated. The outlines of B1, NGC 1333, and L1455 are marked with contours of ^{13}CO $J = 1$–0 line emission taken from Bachiller & Cernicharo (1986).

In Figures 2 and 3 we present the images of the newly found HH objects in the [S II] band. These objects demonstrate a great variety of morphological structures, including knots, jets, and bow shocks, with linear sizes ranging from 0.02 pc (HH 427) to 0.5 pc (a jet composed of HH 432 and HH 433).

HH 426 (Fig. 2*a*) consists of two bright knots and is located in the south of NGC 1333. There are two *IRAS* sources near HH 426, IRAS 03254+3050 and IRAS 03257+3034 (LkHα 325), which are about 9′ northwest and 7′ south, respectively, of HH 426. IRAS 03254+3050 is a Class I object suggested by observations in the *H* and *K* bands (Ladd, Lada, & Myers 1993). A CO outflow was found around LkHα 325 (Bally & Lada 1983). However, the alignment of the two knots of HH 426, which is in the northeast-southwest direction, indicates that neither IRAS 03254+3050 nor IRAS 03257+3034 is the possible exciting

TABLE 2

OBSERVATION LOG

Field	Field Center		Exposure Time (s)		
	α (B1950.0)	δ (B1950.0)	[BATC09]	[BATC10]	[S II]
NGC 1333.....	3 25 29	30 00 09	3 × 300	3 × 300	3 × 1200
B1	3 29 31	31 00 14	3 × 300	3 × 300	3 × 1200
B1 south.....	3 29 32	30 09 56	3 × 300	3 × 300	3 × 1200

NOTE.—Units of right ascension are hours, minutes, and seconds, and units of declination are degrees, arcminutes, and arcseconds.

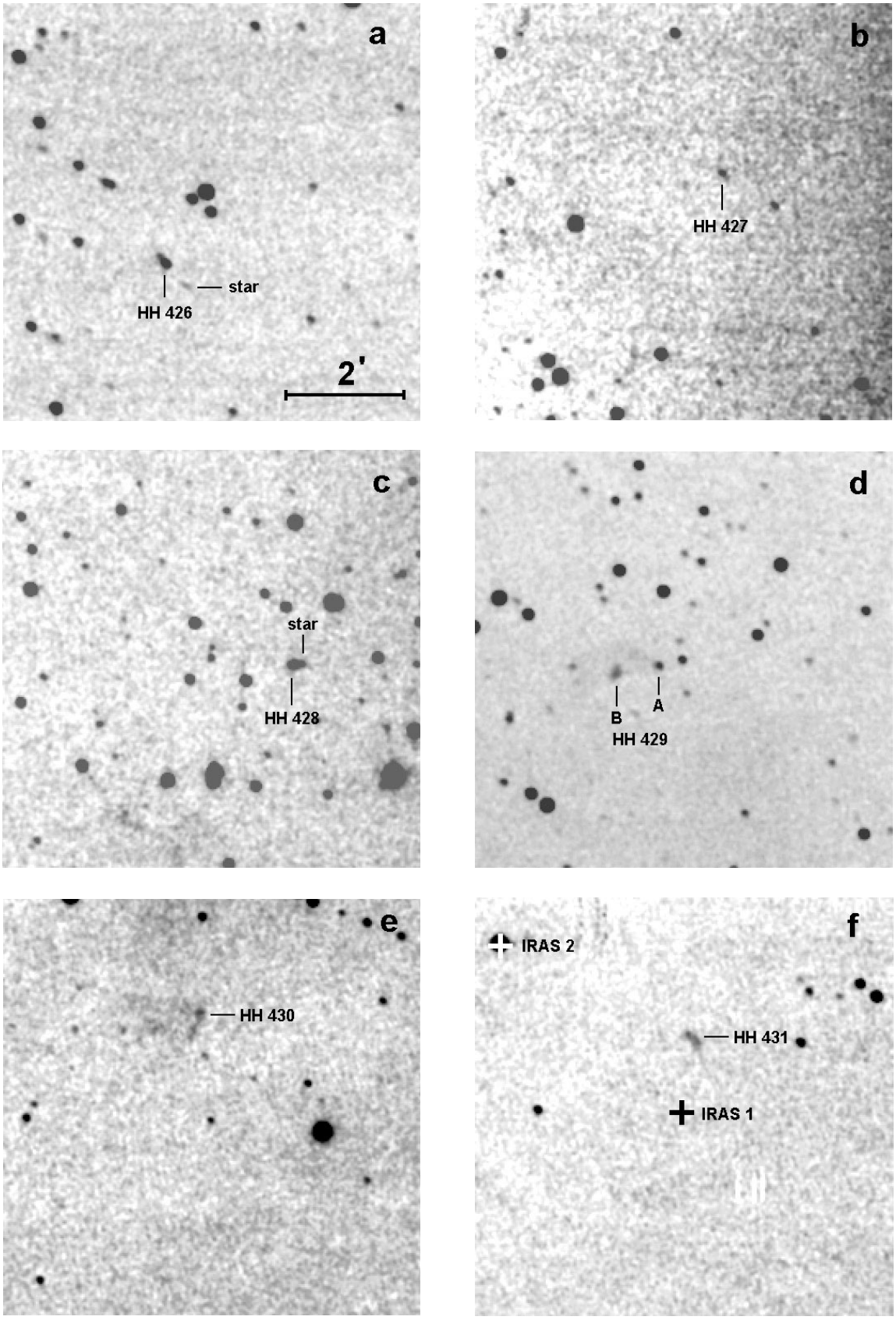

FIG. 2.—[S II] images of the newly discovered HH objects: (*a*) HH 426, (*b*) HH 427, (*c*) HH 428, (*d*) HH 429, (*e*) HH 430, and (*f*) HH 431. All the fields are $7' \times 7'$; north is up, east is to the left, and the scale is shown in (*a*).

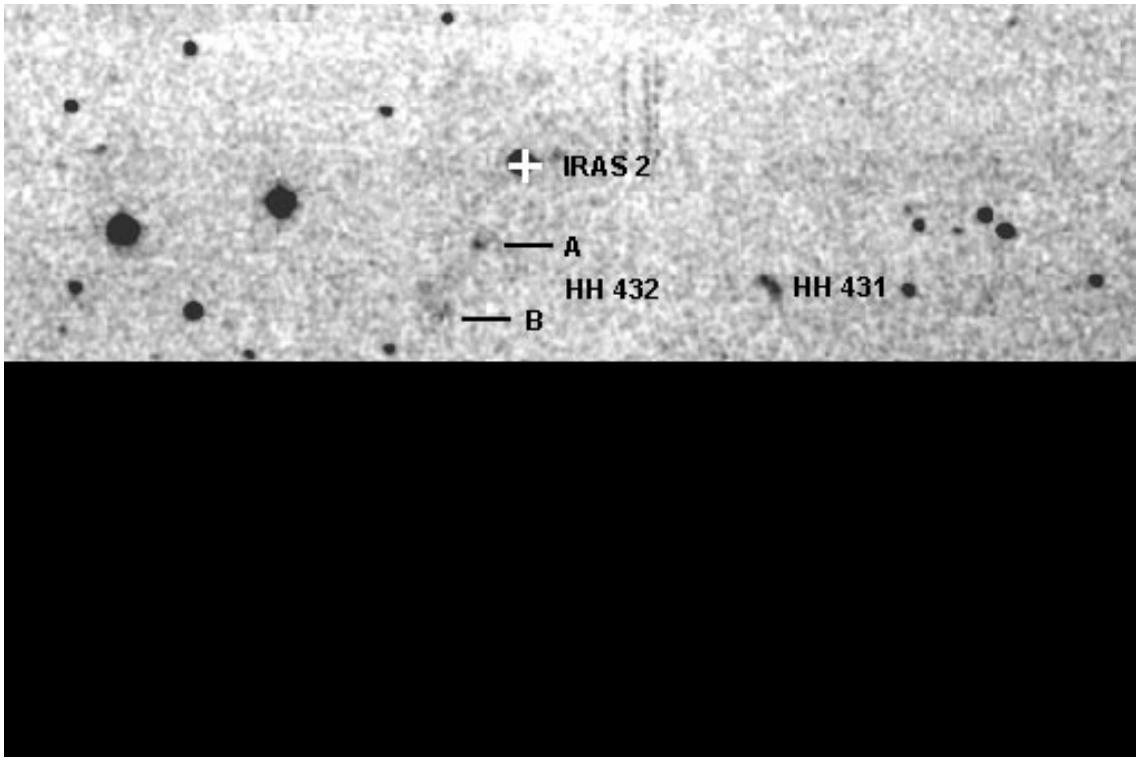

FIG. 3.—[S II] image of the B1 core region where HH 431, 432, and 433 are located. IRAS 03301+3057 ("IRAS 1") and IRAS 03304+3100 (LkHα 327, "IRAS 2") are also marked. The field is 15′ × 10′; north is up and east is to the left.

source of HH 426. We suppose that the faint star (also marked in Fig. 2*a*) 28″ southwest of HH 426 is the exciting source, as judged by its coincidental alignment with the two knots of HH 426.

HH 427 (Fig. 2*b*) is located in the southwest end of the molecular ridge extending from B1 to L1455. It is 5.′3 southeast of IRAS 03271+3013, which is a Class I object (Ladd, Lada, & Myers 1993) associated with a low-mass dense core and a weak molecular outflow (Bachiller, Martin-Pintado, & Planesas 1991). The 1′ × 1′ map centered at IRAS 03271+3013 shows that the outflow is bipolar, oriented in the northeast-southwest direction. Therefore, it seems that HH 427 is not associated with IRAS 03271+3013, and its exciting source is not clear.

TABLE 3

NEW HERBIG-HARO OBJECTS

Object	α (B1950.0)	δ (B1950.0)	Comments
HH 426	3 25 49.30	30 42 06.9	Two knots
HH 427	3 27 33.11	30 11 43.4	Knot
HH 428	3 27 42.39	30 27 50.9	Bar
HH 429A	3 28 42.35	30 59 50.3	Bright knot
HH 429B	3 28 45.84	30 59 43.5	Bright knot
HH 430	3 29 21.71	31 14 31.8	Jet
HH 431	3 30 09.16	30 59 03.5	Bow shock–shaped patch
HH 432A	3 30 27.49	30 59 40.8	Knot
HH 432B	3 30 29.77	30 58 47.3	Group of knots
HH 433A.....	3 30 43.72	30 54 54.5	Knot
HH 433B	3 30 44.37	30 54 58.3	Knot
HH 433C	3 30 44.48	30 55 01.3	Knot
HH 433D	3 30 45.03	30 55 20.1	Knot

NOTE.—Units of right ascension are hours, minutes, and seconds, and units of declination are degrees, arcminutes, and arcseconds.

HH 428 (Fig. 2*c*) is a bright bar connected with a star (the star is also marked in Fig. 2*c*). There are two *IRAS* sources within 10′ of HH 428, IRAS 03275+3020 and IRAS 03276+3022, which are, respectively, 8.′1 southwest and 5.′3 south of HH 428, and are Class I objects according to their *IRAS* fluxes. IRAS 03282+3035, which is 10.′2 northeast of HH 428, drives a high-velocity CO outflow with the redshifted lobe northwest, and the blueshifted lobe southeast (Bachiller, Martin-Pintado, & Planesas 1991). Based on the locations of HH 428 and IRAS 03282+3035 and the orientation of the CO outflow, we conclude that HH 428 is not associated with IRAS 03282+3035. We suppose that HH 428 is driven by the star associated with it.

HH 429 (Fig. 2*d*) consists of two knots, HH 429A and 429B. It is located in the westen edge of B1 cloud. In the vicinity of HH 429 there is neither an *IRAS* source or known CO outflow. HH 430 (Fig. 2*e*) is an optical jet oriented in the northwest-southeast direction with a projected linear size of ∼0.06 pc and a collimation ratio of ∼4. IRAS 03287+3116, a Class II object, is about 7.′6 northwest of HH 430. On the basis of the available data, the exciting sources of HH 429 and HH 430 cannot be identified.

HH 431 (Fig. 2*f*) is a bow shock–shaped patch located near the center of the B1 cloud. The nearby *IRAS* sources, IRAS 03301+3057 ("IRAS 1") and IRAS 03304+3100 (LkHα 327, "IRAS 2"), are also marked in the [S II] image. A CO outflow (size less than 0.03 pc) was found around IRAS 03301+3057 (Bachiller et al. 1990), which is 1.′3 south of HH 431. The orientation of the CO outflow around IRAS 03301+3057 is unknown. Both HH 432 and 433 are located in the east part of the B1 dense core. HH 432 (Fig. 3) consists of two knots, HH 432A and 432B. HH 433 (Fig. 3) consists of four knots, HH 433A–HH 433D. HH 433A,

433C, and 433D constitute a bow shock, with 433B located in the axis of the bow.

The alignment among HH 432A, 432B, HH 433, and IRAS 03304+3100 (LkHα 327) is remarkable (see Fig. 3). This configuration suggests that HH 432 and 433 may constitute a giant, highly collimated jet with a projected linear size of ~0.5 pc and a collimation ratio of ~11, and with IRAS 03304+3100 (LkHα 327) as its driving source. Furthermore, we note that HH 431 and HH 433 are a plausible pair of bow shocks; therefore, it is also possible that they are driven by an unknown exciting source between them.

We acknowledge the staff members of BATC Beijing group for helpful discussions and excellent support. We appreciate Bo Reipurth for assigning HH numbers for our objects and also for his valuable comments. This research was supported by grants from the Natural Science Foundation of China.

REFERENCES

Alten, V. P., Bally, J., Devine, D., & Miller, G. J. 1997, in IAU Symp. 182 Poster Proc., Low Mass Star Formation from Infall to Outflow, ed. F. Malbet & A. Castets (Grenoble: Obs. Grenoble), 51
Aspin, C., Sandell, G., & Russell, A. P. G. 1994, A&AS, 106, 165
Bachiller, R., & Cernicharo, J. 1984, A&A, 140, 414
———. 1986, A&A, 166, 283
Bachiller, R., Martin-Pintado, J., & Planesas, P. 1991, A&A, 251, 639
Bachiller, R., Menten, K. M., & del Rio-Alvarez, S. 1990, A&A, 236, 461
Bally, J., Devine, D., & Reipurth, B. 1996, ApJ, 473, L49
Bally, J., & Lada, C. J. 1983, ApJ, 265, 824
Cohen, M. 1980, AJ, 85, 29
Fan, X., et al. 1996, AJ, 112, 628
Gyulbudaghian, A. L., Glushkov, Yu. I., & Denisyuk, E. K. 1978, ApJ, 224, L137
Haro, G. 1952, ApJ, 115, 572
Herbig, G. H. 1951, ApJ, 113, 697
———. 1974, Lick Obs. Bull., 658
Hodapp, K. W., & Ladd, E. F. 1995, ApJ, 453, 715
Jennings, R. E., Cameron, D. H. M., Cudlip, W., & Hirst, C. J. 1987, MNRAS, 226, 461
Lada, C. J., Alves, A., & Lada, E. A. 1996, AJ, 111, 1964
Ladd, E. F., Lada, E. A., & Myers, P. C. 1993, ApJ, 410, 168
Liseau, R., Sandell, G., & Knee, L. B. G. 1988, A&A, 192, 153
Reipurth, B. 1994, A General Catalogue of Herbig-Haro Objects (Garching: ESO)
Reipurth, B., & Cernicharo, J. 1995, in Circumstellar Disks, Outflows and Star Formation, ed. S. Lízano & J. M. Torrelles (Rev. Mexicana Astron. Astrofis. Ser. Conf. 1) (México, D. F.: Inst. Astron., Univ. Nac. Autonoma México), 43
Sandell, G., Aspin, C., Duncan, W. D., Russell, A. P. G., & Robson, E. I. 1991, ApJ, 376, L17
Sandell, G., Knee, L. B. G., Aspin, C., Robson, I. E., & Russell, A. P. G. 1994, A&A, 285, L1
Schwartz, R. D. 1978, ApJ, 223, 884